Construction and Building Materials 129 (2016) 106–115

Contents lists available at ScienceDirect

Construction and Building Materials

journal homepage: www.elsevier.com/locate/conbuildmat

Quantitative analysis of concrete property under effects of crack, freeze-thaw and carbonation

Yongchun Cheng, Yuwei Zhang, Yubo Jiao *, Jinsheng Yang

College of Transportation, Jilin University, Changchun, Jilin 130025, China

HIGHLIGHTS

- Experiment scheme was designed based on orthogonal method.
- Combined influences of carbonation, F-T cycles, chloride penetration and cracks on concrete properties were investigated.
- Compressive strength of concrete possesses negative correlation with times of F-T cycles.
- Crack width possesses the most significant effect on rebar corrosion.

ARTICLE INFO

Article history:
Received 3 August 2016
Received in revised form 23 October 2016
Accepted 30 October 2016
Available online 4 November 2016

Keywords:
Concrete
Crack
Freeze-thaw cycle
Carbonation
Rebar corrosion
Quantitative analysis

ABSTRACT

Bridge structures are exposed to vehicle loading and aggressive environments, damage of concrete will inevitably occur. In this study, influences of crack, freeze-thaw (F-T) cycling and carbonation on mechanical property and durability of reinforced concrete were investigated. Concrete prism specimens with rebars were prepared. Corresponding experimental arrangement was obtained based on orthogonal design method, and nine groups of reinforced concrete samples were tested. These samples were firstly loaded to produce cracks with different widths. Secondly, they were retained in cyclic F-T testing machine. Spalling mass and compressive strength were measured and evaluated for concrete under different crack widths and F-T cycles. Then concrete samples were exposed to carbon dioxide (CO_2) gas pressure. Finally, chloride induced corrosion of rebar was tested and combined effects of crack, F-T cycling and carbonation on rebar corrosion were demonstrated based on range analysis (RA), analysis of variance (ANOVA) and Spearman's rank correlation coefficient method (SRCCM), respectively. The results reveal that crack and F-T cycles all increase the spalling mass of concretes, whereas reduce their compressive strength. Crack presents more significant effect on rebar corrosion compared with F-T cycles and carbonation.

1. Introduction

Reinforced concrete (RC) is one of the most widely used materials for bridge construction. Compressive strength of concrete is an important factor for mechanical performance of RC bridge, while corrosion of rebar is an important problem which reduces its durability [1,2]. In practice, effects of penetration of chloride ions, carbonation of concrete, F-T cycles or external loads can cause concrete damage, corrosion of rebar, and eventually collapse of bridge [3]. In general, the high alkalinity of concrete pore solution can be used as passive layer to protect rebar against corrosion. However, the passive layer will be weakened because of effects from penetration of chloride ions, carbonation of concrete and F-T cycles. As the corrosion proceeds, rust appears. Rust possesses greater volume, which induces cracks of concrete cover. Meanwhile, reinforced concrete will form internal cracks because of material shrinkage and repeated loading. These phenomena will threaten the safe operation of bridge [4,5]. Therefore, investigations on mechanical property and durability of structure in aggressive environments are important to be pursued.

Carbonation of concrete occurs naturally in RC bridge at a rather low yet invasive rate, which is the chemical reaction of portlandite and calcium hydroxide ($Ca(OH)_2$) in cement with CO_2 [6]. Some comprehensive reviews of concrete carbonation have been given on mechanism [7,8], modeling [9], mitigation [10] and industry implication [11]. Besides, the reaction of concrete carbonation depletes the hydroxyl ions (OH^{-1}) and reduces the pH of concrete. It makes steel bar lose its stable alkaline condition and leads to a

* Corresponding author at: No. 5988, Renmin Street, City of Changchun 130025, China.
E-mail address: jiaoyb@jlu.edu.cn (Y. Jiao).

http://dx.doi.org/10.1016/j.conbuildmat.2016.10.113
0950-0618/

high steel corrosion rate under the action of unfavorable ions [12]. Current researches reveal that carbonation influences the diffusion of chloride ions, and then the rebar corrosion caused by chloride ions [13–15].

F-T cycling is one of the most harmful phenomena for concrete, which has been investigated for many years. The main mechanisms of F-T damage have been identified [16]. F-T cycling can lead to not only superficial spalling, but also serious internal cracking. Consequently, the elastic modulus and compressive strength of concrete decrease and penetration of chloride ions increases [17–19]. Therefore, concrete loses its resistance to mechanical loading and harmful environmental conditions.

In addition, chloride penetration-induced corrosion of rebar in RC concrete is a serious threat to durability of structures [20]. Once the chloride concentration around the surface of rebars exceeds a certain threshold value, the rebars will undergo the depassivation process. Corrosion process is initiated when the chloride ions (Cl^-), oxygen (O_2) and water are sufficient [3]. Lambert et al. [21] demonstrated that chloride ions deteriorate durability of RC structures because of leading to steel corrosion. Experimental investigation by Shaheen and Pradhan [22] revealed that the range of passive region of steel reinforcement decreases with increasing in free chloride concentration for concrete made by both ordinary Portland cement and Portland pozzolana cement.

Furthermore, Cracks cannot be avoided for a real structure, which can be caused by shrinkage, thermal gradients, corrosion of rebar, mechanical loading, etc. These cracks often become preferential paths for the ingress of external agents and lead to degradation of both durability and carrying capacity of structure [23]. Ji et al. [24] demonstrated that cracks will allow more penetration substance, such as CO_2 and chloride ions to invade into pore solution. It accelerates the carbonation process and leads to more and deeper cracks. Zhang et al. [25] found that existence of cracks changes mechanical behavior and reduces load carrying capacity of structure. Cracks also decrease distance between steel bar and external environment at the places of cracks. This situation increases the probability of steel corrosion and deteriorates durability of RC structures.

A large number of researches have been conducted, most of which focus on a single factor that influence properties of RC structures. However, structures usually suffer from a couple effects of multi-factor in natural environment. The influences are complex and synergetic instead of simple superposition by each single factor. There is a rapidly increasing amount of studies on concrete properties with multi-factor. Niu et al. [26] conducted an experimental study on concrete damage and chloride penetration under effects of carbonation and F-T cycles. Zhu et al. [3] investigated the combined effects of carbonation and chloride ingress on concrete. Kuosa et al. [27] demonstrated the synergetic effects of freeze-thaw, carbonation and chlorides on concrete deterioration. Wittmann et al. [28] examined chloride corrosion resistance and rate of chloride diffusion of concrete under alternate actions of freeze-thaw cycles and carbonation. However, many combined aspects have not been demonstrated through experimental and analytical methods in sufficient details.

In this paper, the combined influences of carbonation, F-T cycles and cracks on mechanical property and durability of ordinary Portland concrete were investigated. Experimental scheme was determined through orthogonal design. Nine groups of RC samples were tested according to the order of pre-crack, cyclic F-T, carbonation and chloride-induced rebar corrosion. Quantitative analyses including RA, ANOVA and SRCCM were conducted to evaluate and compare the effects of crack, freeze-thaw and carbonation on concrete property, respectively.

2. Materials and experiments

2.1. Materials and mixture

Q235 steel round bars with diameter 8 mm are cut into 580 mm long. Firstly, the steel bars are polished with grit silicon carbide (SiC) emery paper in order to guarantee no pit corrosion on them. Subsequently, steel bars are cleaned using 12% hydrogen chloride (HCl) solution and then immersed into $Ca(OH)_2$ solution to neutralize residual HCl liquid. Then, ethanol and acetone treatments are used to degrease surfaces of steel bars according to GB/T 50082-2009 [29]. Finally, steel bars are flushed cleanly with clear water and put into drying device at 20 °C for 4 h. Each steel bar is weighed to obtain the initial mass using sensitive balance.

PO 42.5 type Portland cement confirming the requirements of GB175-2007 [30] is used in this study. Crushed stone with diameters ranging from 2.36 mm to 26.5 mm and natural sand with fineness modulus of 2.7 are adopted as coarse and fine aggregates, respectively. The mixture proportions of concrete are listed in Table 1. Slump result of concrete is tested to be 40 mm, which indicates that the mixture is with favorable cohesiveness and meets the requirement of GB 50164-2011 [31].

2.2. Specimen preparation

Specimen used in this study is composed of concrete and two steel bars. Dimensions of specimen and relative positions between concrete and rebar are shown in Fig. 1. The concrete mixtures were prepared in the laboratory by a pan mixer. Prisms of $300 \times 150 \times 150$ mm were cast in steel moulds and compacted by vibrating table. They are allowed to cure at 20 °C and 95% relative humility (RH) and removed from the moulds after 24 h curing. Besides, waterproofing treatments of smudging the silicone sealant on steel bars and binding them up with waterproof tape must be used for the exposed parts of steel bars to resist the corrosion from water and oxygen in curing room (shown in Fig. 2). All specimens are cured under normal curing condition (20 °C and 95% RH) for 28 days before further tests.

2.3. Experimental methods

2.3.1. Scheme design

Orthogonal design of experiment is an effective approach to deal with the test including multiple factors and levels, which can reduce the number of required experiments and achieve reasonable results [32]. It has been adopted by many researchers to improve work efficiency and obtain the optimum level group [32–35]. In this study, three factors prevalent in concrete situated in higher latitudes including crack width, F-T cycle and carbonation time are considered, and each one has three levels. The choices of values for three factors are essential to determine the influence degrees of factors. According to the statistics of China Meteorological Administration (CMA), average times of F-T cycles are 74 in one year for central south, north and northeast regions of China, whose extreme low temperatures range from −40 °C to −10 °C. Based on current research [36], one time of fast F-T cycle in indoor test used in this study is equivalent to 15 times of natural F-T

Table 1
Mixture proportions of concrete.

Materials	Nominal proportions (kg/m^3)
Cement	349
Water	185
Fine aggregate	517
Coarse aggregate	1269

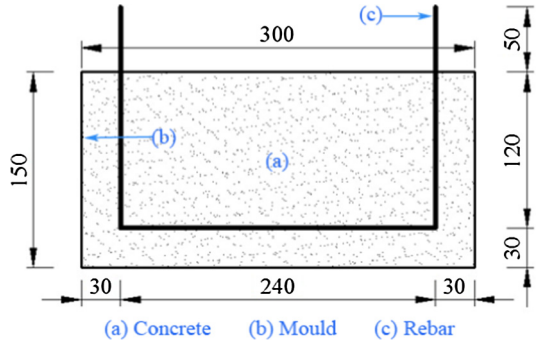

Fig. 1. Specimen dimension and rebar arrangement.

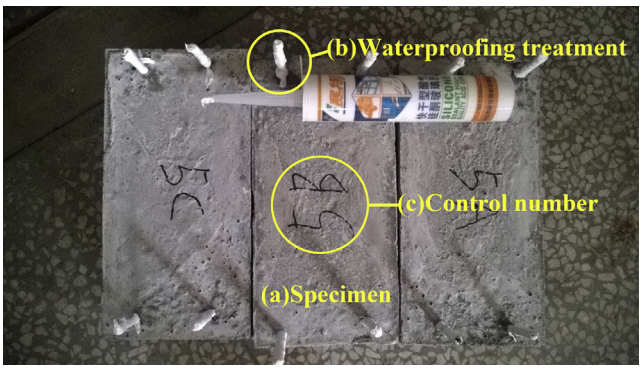

Fig. 2. Waterproofing treatment of steel bar.

cycles. Besides, service life of bridge is assumed to be 30 years in this study. So the reasonable times of fast F-T cycles in indoor test should be 30 × 74/15 = 148. For carbonation time, the natural CO_2 concentration is 0.039%, while it is 20% in accelerated carbonation test chamber used in this study [29]. One day accelerated carbonation test is equivalent to 20%/0.035%/365 = 1.56 year's natural carbonation. So the reasonable days of accelerated carbonation in experiment should be 30/1.56 = 19.23 days. According to the standard JTG D62-2004 [37], the maximum allowed crack width of reinforced concrete bridge in China is 0.2 mm. Therefore, the range of crack widths is set to be 0–0.2 mm; it is 0–150 times for F-T cycles and 0–20 days for carbonation time in this study.

An orthogonal design table $L_9(3^4)$ is used, which can reduce the number of test cases from 27 to 9. Three factors and corresponding levels used in this paper are listed in Table 2. Groups of specimens obtained by orthogonal design table $L_9(3^4)$ are shown in Table 3.

According to Table 3, all prepared specimens are taken out of the curing room and divided into nine groups. Three specimens are included in each group, which can be numbered by 1A, 1B, 1C to 9A, 9B, 9C (as shown in Fig. 2) in order to demonstrate the experimental results conveniently.

In order to investigate the influences of crack, F-T cycling and carbonation on mechanical property and durability of reinforced concrete, experimental procedure is determined and shown in Fig. 3. In this figure, "Activate" and "passivate" represent corresponding experiment is conducted and not conducted, respectively. "Test indicators" include mass of surface scaling, compressive strength and rebar corrosion in this study. "Test group" denotes that the test indicators need to be tested and calculated at this time point. As shown in Fig. 3, specimens in groups 2, 3, 4, 5, 7 and 9 are firstly loaded to produce cracks. Secondly, specimens in groups 4 to 9 are retained in cyclic F-T testing machine for F-T tests. After that, mass of surface scaling and compressive strength of samples in groups 7, 8 and 9 with 150 times of F-T cycles are measured at 25 times interval. Then specimens in groups 2, 3, 5, 6, 8 and 9 are exposed to CO_2 gas pressure in an accelerated carbonation test chamber. Finally, specimens in groups 1 to 9 are performed accelerated galvanic corrosion experiment after immersing them into sodium chloride (NaCl) solution, chloride induced corrosion ratio of rebar is calculated after test.

Table 3
Experimental groups designed by orthogonal method.

Factors	Crack width (mm)	F-T cycles (times)	Carbonation time (days)
Group 1	0.00	0	0
Group 2	0.10	0	10
Group 3	0.20	0	20
Group 4	0.10	75	0
Group 5	0.20	75	10
Group 6	0.00	75	20
Group 7	0.20	150	0
Group 8	0.00	150	10
Group 9	0.10	150	20

2.3.2. Crack inducing

The specimen is supported on two concrete prisms, and force is applied to the specimen through a half-cylinder iron indenter as shown in Fig. 4. Distance between two supporting points at the bottom of specimen is controlled to be 220 mm. The loading rate is controlled at 10kN/min at the beginning. Loading rate is reduced to 2kN/min when the load on specimen reaches 50kN. During loading process, crack widths at the bottom of specimen are continuously detected using crack width recorder at interval of 0.5 min. Crack width is decided as the average of measurement values from 5 measured points. When the crack width reaches target value, loading is terminated. If crack width does not satisfy experimental requirement, loading rate is lowered and the crack width is checked frequently with each additional 0.5kN until the crack width meeting requirements. The difference between the measured crack width and that designed in orthogonal method should not be larger than 5%. In this study, the crack only appears at the bottom of specimen.

2.3.3. Freeze-thaw cycle test

Cyclic F-T loading is performed on concrete specimens for groups 4 to 9. Process of F-T experiment is designed and rapid cyclic F-T testing machine is used in reference with the requirements of GB/T 50082-2009 [29]. Temperature range is controlled from 5 °C to −20 °C. One complete F-T cycle lasts 4 h and 150 times of F-T cycles take about 25 days. Specimens are placed into rubber boxes filled with water during F-T cycles. Liquid with high rate specific heat capacity (75 wt.% ethylene glycol) flows in circular

Table 2
Factors and levels for crack width, F-T cycles and carbonation time in the test.

Factors	Units	Level 1	Level 2	Level 3
Crack width	mm	0.00	0.10	0.20
F-T cycles	times	0	75	150
Carbonation time	days	0	10	20

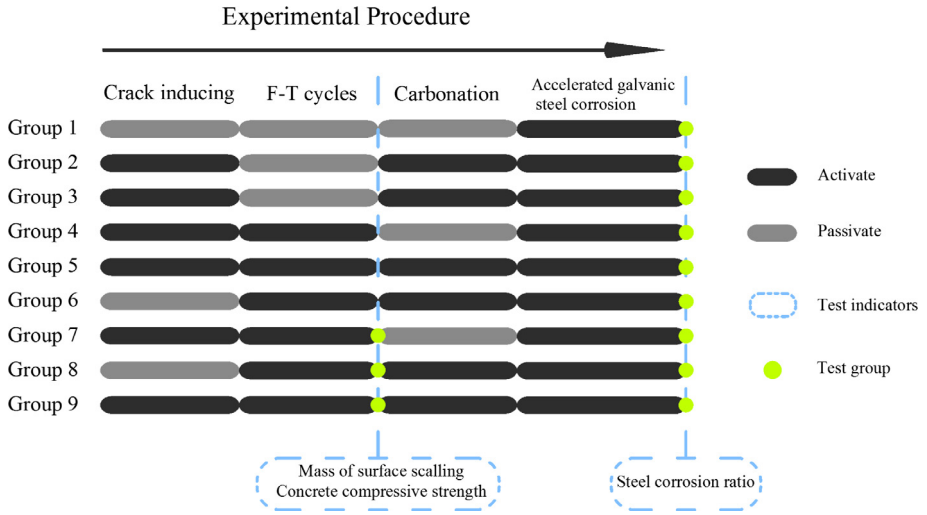

Fig. 3. Experimental procedure for property evaluation of concrete.

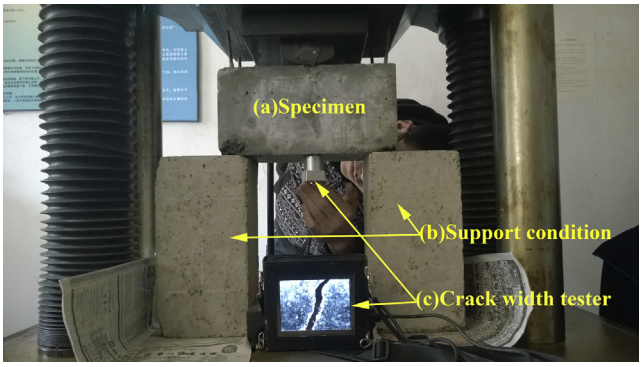

Fig. 4. Crack inducing through loading.

fashion around the rubber boxes, which can realize the freezing and thawing for water and specimens.

According to the testing process shown in Fig. 3, compressive strength will be measured for specimens after cyclic F-T loading, then the carbonation and accelerated steel corrosion tests. In this study, the specimens should be nondestructive when carbonation and accelerated steel corrosion tests are conducted. However, traditional testing method for concrete strength using compression machine will destroy the specimens. Therefore, ultrasonic-rebound nondestructive method is adopted to test the specimens' compressive strength after F-T cycles. And the rebound values and corresponding ultrasonic wave velocities of each specimen are tested after each 25 F-T cycles.

According to CECS 02: 2005 [38], compressive strength can be calculated by

$$f_{cu}^{c} = 0.0162 v^{1.656} R^{1.41} \quad (1)$$

where f_{cu}^{c} is compressive strength; v and R are ultrasonic wave velocity and rebound value, respectively.

In addition, mass of concrete surface scaling is also tested. Corresponding change ratio can be calculate by

$$\omega_c = (m_{c0} - m_{c1})/m_{c0} \quad (2)$$

where ω_c is mass change ratio of concrete surface scaling; m_{c0} is initial mass of specimen after drying at 60 °C for 24 h in the drying oven before F-T cycle; m_{c1} is mass of specimen after F-T cycles and drying at 60 °C for 24 h in the drying oven.

In this study, compressive strength and surface scaling for specimens in groups 7, 8 and 9 with 150 times of F-T cycles were tested and calculated at 25 times interval. Average value for three specimens in each group is regarded as representative one for performance evaluation.

2.3.4. Carbonation

According to Table 3, groups 2, 3, 5, 6, 8 and 9 are needed for carbonation test. In order to ensure samples in these groups with the same initial state before carbonation, samples in groups 2, 3, 5 and 6 are dried at 60 °C for 24 h in an oven before putting into carbonation test chamber. For samples in groups 8 and 9, they have been dried at 60 °C for 24 h before surface scaling examination, which can be used for carbonation test directly. According to standard GB/T 50082-2009 [29], specified samples in control groups are put into an accelerated carbonation test chamber with (20 ± 2)% CO_2 concentration, (20 ± 2)°C temperature and (70 ± 5)% relative humidity. Other specimens no need for carbonation would be placed at the laboratory until carbonation test being completed. In this study, carbonation effect is one of the influence factors on rebar corrosion in chloride salt environment. And the action of CO_2 on reinforcement concrete structure should be in one-dimension. Therefore, specimens are sealed around with paraffin except bottom and top sides. Then, they are placed in the concrete carbonation test chamber. In order to reduce the influence of concrete carbonation on nondestructive strength evaluation, the carbonation experiment should be conducted after F-T cycles experiment and compressive strength test.

2.3.5. Electrochemical accelerated steel corrosion

The electrochemical nature of corrosion means that electrochemical techniques can be used to accelerate the corrosion behavior of steel bars in concrete. In general, it will take long time to observe the effect on concrete due to the slow corrosion process of chloride ions. However, electrochemical accelerated corrosion shows a more effective way to accelerate the corrosion process of chloride ion [13]. The electrochemical accelerated steel corrosion device and circuit connection are displayed in Fig. 5.

Nine groups of specimens are immersed into 6% NaCl solution and used for corrosion experiment after crack inducing, F-T cycles and carbonation. Firstly, the waterproof layers on steel bars are removed before test. Then, the anode of direct current (DC) regulated power supply is connected with four rebars in parallel mode, while the cathode is connected with copper sheet immersed into

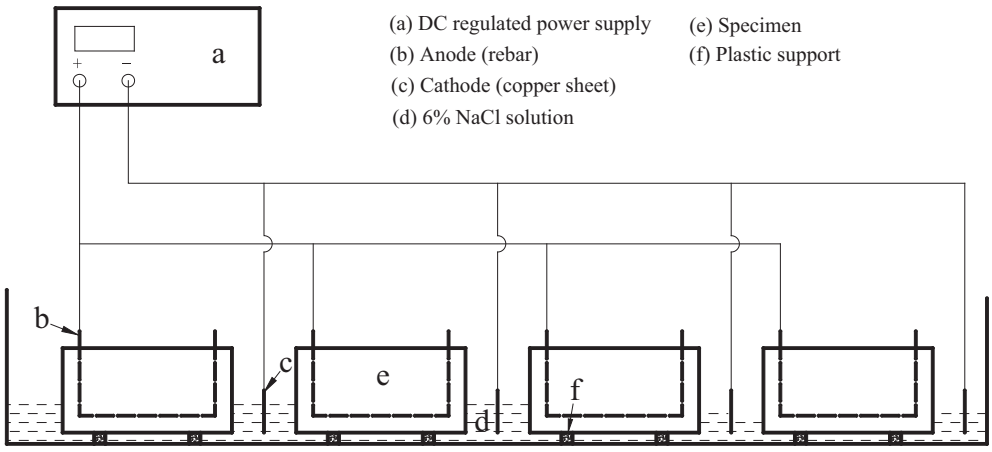

Fig. 5. Sketch of experimental setup for electrochemical accelerated steel corrosion.

NaCl solution also in parallel mode. Finally, the system is electrified for 24 h. The specimens should be immersed into chlorine salt solution for 7 days to ensure that the chloride ions can penetrate into interior of concrete under capillary action. Meanwhile, the current density of steel is not higher than 30 A/m^2, each branch current is set as 0.12 A and voltage is 16.3 V.

After designed electrochemical experiment, concrete specimens should be broken with compression machine and corroded steel bars are taken out. The concrete dust on the surface of corroded steel bars is removed and steel bars from all control groups are placed into 12% HCl solution to dissolve the rust, and then put them into $Ca(OH)_2$ solution to neutralize the residual HCl liquid. Steel bars are flushed cleanly with clear water and put into drying device at 20 °C for 4 h. Mass of steel bars are tested using sensitive balance after removing rust, the steel corrosion ratio can be calculated as

$$\omega_s = (m_{s0} - m_{s1})/m_{s0} \quad (3)$$

where ω_s is steel corrosion ratio; m_{s0} is the initial mass of steel bars and m_{s1} is the mass of steel after removing rust.

3. Results and discussion

3.1. Mass of concrete surface scaling

The frozen layer forms firstly on the bare concrete surface due to the effects of complex F-T environments and get deeper gradually. So the mass of concrete surface scaling represents the progressive failure of concrete and it is the external behavior of F-T damage. The mass of concrete surface scaling for groups 7–9 after each 25 times of F-T cycles have been tested, corresponding change ratio ω_c are calculated and shown in Fig. 6.

As can be seen from Fig. 6, the mass change ratio of concrete surface scaling increases with the increasing of F-T cycles. It represents the damage of concrete occurs gradually under F-T effects. However, the increasing rate for mass of concrete surface scaling is decreasing along with the increasing of F-T cycles. Furthermore, mass change ratio increases with increasing of crack width for concrete with the same F-T cycles, which reveals that crack width has enhancement effect on F-T cycling caused damage of concrete.

3.2. Compressive strength of concrete

In this study, rebound and ultrasonic velocity values of specimens in groups 7 to 9 after each 25 times of F-T cycles are tested.

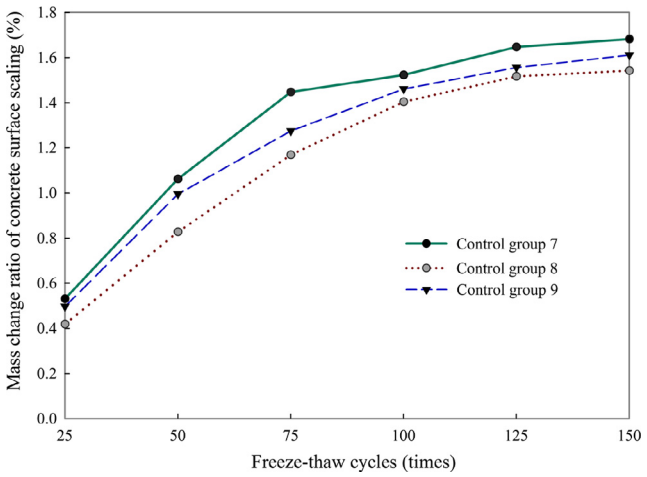

Fig. 6. Mass change ratio of concrete surface scaling for groups 7–9 after F-T cycles.

Corresponding compressive strengths are calculated according to Eq. (1). The results are shown in Fig. 7.

From Fig. 7, it can be concluded that concrete compressive strength is decreasing with the increasing of F-T cycles. The concrete compressive strength decreases by 47.4% for group 7 after

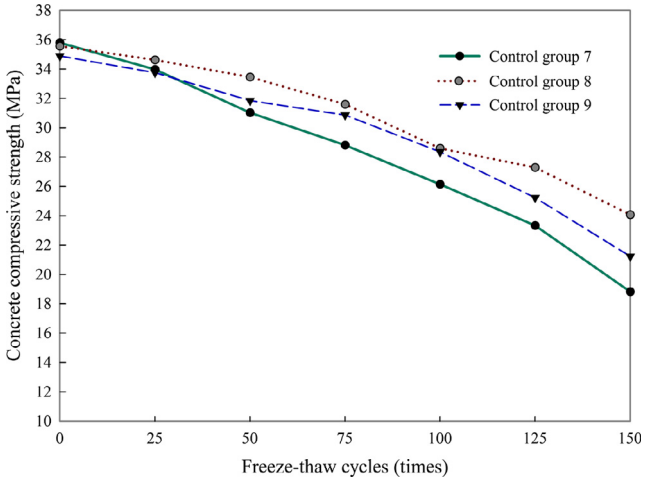

Fig. 7. Compressive strength of concrete for groups 7–9 after F-T cycles.

150 times of F-T cycles, and they are 32.3% and 39.1% for groups 8 and 9, respectively. Meanwhile, it can also be found that the greater induced crack width is, the higher decreasing rate of compressive strength caused by F-T cycles becomes. The reason for the loss of concrete compressive strength lies in that pore solutions in concrete undergo repeated freezing and thawing after each F-T cycles. Concrete often suffers from sustainable extended internal micro-cracks, surface scaling and loss of cover thickness on macroscopic scale.

3.3. Steel bar corrosion ratio

Steel corrosion has occurred after the designed electrochemical experiment, which is shown in Fig. 8. Serious steel corrosion can be observed at the place where cracks exist and uniform corrosion presents at those without crack. And it can also observe that the pit corrosion appears on the surface of steel bars and the rust has already penetrated in concrete.

Steel bar corrosion ratio for each specimen is calculated by Eq. (3). Average value for three specimens in each group is regarded as representative value and listed in Table 4. Corresponding standard deviations are also calculated. The results can be used to analyze the influences of F-T cycles, carbonation and crack width on durability of reinforced concrete. Comparative evaluations are conducted based on RA, ANOVA and SRCCM, respectively.

3.3.1. Range analysis (RA) method

RA is an easy, intuitionistic, and effective method for orthogonal experiment. This method can quantitatively analyze the sensitivity of each factor [39]. In order to analyze the significant influence of single-factor based on RA method, range (R) of experimental results can be calculated by

$$R_j = \max\left(\overline{K_{j1}}, \overline{K_{j2}}, \ldots \overline{K_{ji}}, \ldots, \overline{K_{jm}}\right) - \min\left(\overline{K_{j1}}, \overline{K_{j2}}, \ldots \overline{K_{ji}}, \ldots, \overline{K_{jm}}\right) \quad (4)$$

where m is the number of levels, which is three in this paper. R_j is the range for factor j, which represents the influence degree of experimental results under different levels. The greater R is, the more sensitive the factor is. $\overline{K_{ji}}$ is the average value of ARSC for factor j at level i ($i = 1, 2, \cdots m$), which can be obtained by

$$\overline{K_{ji}} = K_{ji}/m \quad (5)$$

here K_{ji} is the sum of all the corresponding ARSC values for factor j at level i ($i = 1, 2, \ldots m$). K_{ji} and $\overline{K_{ji}}$ are process indicators for the calculation of R_j.

Process indicators and results of range analysis in this study are listed in Table 5.As can be seen from Table 5, three factors all contribute to the corrosion of steel bars in concrete and the influence degree of corrosion increases with increasing of factor levels. According to range results, R of crack width is larger than that of other factors. Therefore, the variation of crack width has the greatest effect on rebar corrosion. Meanwhile, the influence degrees of three factors on rebar corrosion can also be ranked in the following order: crack width, F-T cycles and carbonation. Therefore, existence of crack is the most harmful factor in this study that can cause steel corrosion.

Fig. 8. Corroded rebar after electrochemical experiment.

3.3.2. Analysis of variance (ANOVA) and post hoc multiple comparisons

3.3.2.1. ANOVA. RA method cannot evaluate experimental errors and take full advantage of information provided by experimental data. ANOVA is the statistical method most commonly used for analyzing the contribution of each factor and factor interaction of experimental results. It can take advantage of sums of squares to separate the overall variance in the response into variances which are caused by measurement error and processing parameters [40]. In this study, ANOVA and F-tests are conducted to determine statistically significant process parameters and present contribution of influence factors on rebar corrosion.In ANOVA, square of deviance SS_j can be calculated by

$$SS_j = \frac{1}{r}\sum_{j=1}^{r}\left(\sum_{i=1}^{m} y_{ji}\right)^2 - \frac{1}{n}\left(\sum_{j=1}^{r}\sum_{i=1}^{m} y_{ji}\right)^2 \quad (6)$$

where m, n and r are the number of levels, control groups and factors, respectively. y_{ji} is experimental results of level i for factor j.The error square of deviance SS_e is given by

$$SS_e = \sum_{j=1}^{r}\sum_{i=1}^{m} y_{ji}^2 - \frac{1}{n}\left(\sum_{j=1}^{r}\sum_{i=1}^{m} y_{ji}\right)^2 - \sum_{j=1}^{r} SS_j \quad (7)$$

And the estimate of variance can be calculated by

$$MS_j = SS_j/d_{f_j} \quad (8)$$

$$MS_e = SS_e/d_{f_e} \quad (9)$$

where MS_j and MS_e are the estimate of variance for factor j and error, respectively. d_{f_j} and d_{f_e} are corresponding degrees of freedom, which can be obtained by

$$d_{f_j} = d_{fe} = m - 1 \quad (10)$$

F-Value can be calculated by

$$F_j = MS_j/MS_e \quad (11)$$

Results of ANOVA in this study are listed in Table 6.F-Value is used to determine whether the factor means are equal or not. The larger F-Value is, the higher effect of factor is. In Table 6, F-T cycles, carbonation and crack action are marked with A, B and C, respectively. It can be found that $F_A > F_{0.01}$, $F_C > F_{0.01}$ and $F_{0.05} < F_B < F_{0.01}$. The probability is 99% that factors of F-T cycles and cracks possess significant effects on rebar corrosion. The probability is 95% that factor of carbonation is the significant influence of corrosion.

According to ANOVA analysis, it is more likely that crack width and F-T cycles have statistically significant effects on steel corrosion, but this does not mean that their effects are with larger magnitude [41]. Therefore, Turkey's HSD (honest significant difference) test is used to perform post hoc multiple comparisons, which can more favorably determine the significant effects of influence factors on rebar corrosion. In addition, regression analysis is also conducted to determine the gradient of the regression line for steel corrosion effect as a function of each factor.

Table 4
Average ratio of steel corrosion (ARSC) and corresponding standard deviation for each group.

Group No.	1	2	3	4	5	6	7	8	9
ARSC (%)	5.31	8.52	11.62	8.56	11.97	7.55	13.26	9.41	11.48
Standard deviation	0.57	0.56	0.76	0.65	0.48	0.35	0.60	0.44	0.48

Table 5
Process indicators and results of range analysis for influence factors.

Factors	Crack width (mm)	F-T cycles (times)	Carbonation time (days)	ARSC (%)
Group 1	0.00	0	0	5.31
Group 2	0.10	0	10	8.52
Group 3	0.20	0	20	11.62
Group 4	0.10	75	0	8.56
Group 5	0.20	75	10	11.97
Group 6	0.00	75	20	7.55
Group 7	0.20	150	0	13.26
Group 8	0.00	150	10	9.41
Group 9	0.10	150	20	11.48
K_{j1}	22.27	25.45	27.13	
K_{j2}	28.56	28.08	29.90	
K_{j3}	36.85	34.15	30.65	
$\overline{K_{j1}}$	7.42	8.48	9.04	
$\overline{K_{j2}}$	9.52	9.36	9.97	
$\overline{K_{j3}}$	12.28	11.38	10.22	
R_j (%)	4.86	2.90	1.18	

Table 6
Three-factor ANOVA and correlation level on rebar corrosion.

Source of variance	Symbol	SS	d_f	MS	F-Value	$F_{0.05}$	$F_{0.01}$	Significance
F-T cycles	A	13.27	2	6.64	110.60	19	99	**
Carbonation	B	2.29	2	1.15	19.10			*
Crack width	C	35.65	2	17.83	297.10			**
Error		0.12	2	0.06				

* Correlation is significant at the 0.05 level.
** Correlation is significant at the 0.01 level.

3.3.2.2. Turkey's HSD test. Turkey's HSD test is a single-step multiple comparison procedure and statistical test. It can be used on raw data or in conjunction with an ANOVA to find means that are significantly different from each other [42]. In Turkey's HSD test, HSD value is the critical index to judge the significant effect of factor. HSD critical value at α level can be calculated by

$$HSD_\alpha = q_\alpha(m, d_{f_j}) \times \sqrt{\frac{MS_e}{n}} \tag{12}$$

where $q_\alpha(m, d_{f_j})$ is studentized range; α is significant level; m is the number of levels in each factor; d_{f_j} is number of degrees of freedom; MS_e is the estimate of variance of error.In this study, the range value $\overline{K_{j3}} - \overline{K_{j1}}$ of factor j is calculated and compared with HSD_α. If $(\overline{K_{j3}} - \overline{K_{j1}}) > HSD_\alpha$, factor j has a significant effect on steel corrosion. Results of Turkey's HSD test are listed in Table 7.As can be seen from Table 7, range values of crack width and F-T cycles are larger than $HSD_{0.01}$, which reveal that crack width and F-T cycles present significant effects at 0.01 level. Range value of carbonation is between $HSD_{0.05}$ and $HSD_{0.01}$, which means that carbonation has significant effects at 0.05 level. Moreover, range value of crack width is the largest one. The results of Turkey's HSD test reveal that crack width possesses greater effect on steel corrosion.

3.3.2.3. Regression analysis. Regression analysis is conducted to quantitatively analyze and compare the effects of crack width, F-T cycles and carbonation on steel corrosion by calculating the regression coefficients (gradient of the regression line for steel corrosion effect as a function of three factors). Considering that the values of factors and ARSC have different units, the original data (shown in Table 5) need to be standardized. Z-score method is adopted for standardization, which can be calculated by

$$z_i = \frac{x_i - \mu}{\sigma} \tag{13}$$

Table 7
Turkey's HSD test results for influence factors.

Factor	MS_e	$q_{0.05}(3,2)$	$q_{0.01}(3,2)$	$\overline{K_{j3}} - \overline{K_{j1}}$	$HSD_{0.01}$	$HSD_{0.05}$	Significance
F-T cycles	0.06	8.28	19.00	2.90	2.68	1.17	**
Carbonation				1.18			*
Crack width				4.86			**

* Correlation is significant at the 0.05 level.
** Correlation is significant at the 0.01 level.

where x_i and z_i are data before and after standardization, respectively; μ and σ are the mean value and standard deviation, respectively.The normalized values of factors and ARSC and corresponding K_{ji}, $\overline{K_{ji}}$ are calculated and listed in Table 8.The least squares method is used for regression analysis. Three levels of each factor are treated as independent variables and corresponding $\overline{K_{ji}}$ $(i = 1, 2, \ldots m)$ are dependent variables. The calculated regression coefficients for three factors are listed in Table 9.

In Table 9, crack width has the largest regression coefficient, which reveals that the magnitude of its influence is the biggest. Therefore, crack width presents the most significant effect on steel corrosion in this study.

3.3.3. Spearman's rank correlation coefficient method (SRCCM)

RA method and ANOVA are standard methods used in orthogonal test. These two methods just consider the factors data (second to forth columns in Table 3) as "signs" instead of independent data associated with experimental results. So the factors data are not calculated with experimental results in these two methods. In order to analyze the correlation between 3 factors with steel corrosion in another way, data of levels for each factor are treated as sets of independent variables X and experimental results are treated as sets of dependent variable Y. Therefore, correlations between average ratio of steel corrosion with each of three factors can be evaluated based on SRCCM. This method is a numerical measure that quantifies the extent of statistical dependence between pairs of observations. Spearman's correlation is nonparametric that its exact sampling distribution can be obtained without requiring knowledge of the joint probability distribution of X and Y, which has a wide application range and fits well with the calculation of correlation coefficient.

In the calculation of SRCCM, the correlation coefficient between independent variable X and dependent variable Y can be calculated according to the following process.

Step 1: data in X are sorted. A new set x_i is created and assigned the ranked values 1,2,3,. . .,n. While there are some same data in X, the rank value of them are the same and calculated by

$$x_i' = \frac{1}{n}\sum_{i=1}^{n} x_i \tag{14}$$

where x_i', x_i, n are new ranked value of the same data, original ranked value of the same data, number of the same data in X, respectively.

Table 9
Regression coefficients for influence factors.

Factor	F-T cycles	Carbonation	Crack width
Regression coefficient	0.50	0.20	0.83

Step 2: data in Y are sorted. A new set y_i is created and assigned the ranked values 1,2,3,. . .,n. While there are some same data in Y, the rank value of them are the same and calculated by

$$y_i' = \frac{1}{n}\sum_{i=1}^{n} y_i \tag{15}$$

where y_i', y_i, n are new ranked value of the same data, original ranked value of the same data, number of the same data in Y, respectively.

Step 3: Set d_{Y,X_i} is calculated to represent the differences between two rank columns (x_i and y_i).

Step 4: Set $(d_{Y,X_i})^2$ is calculated to represent the square value of d_{Y,X_i}.

Spearman's rank correlation coefficient ρ can be computed by

$$\rho = 1 - \left[6\sum_{i=1}^{N}(d_{Y,X_i})^2 / N\left(N^2 - 1\right)\right] \tag{16}$$

where N is number of data in each set. In this study, N = 9.Comparison between critical value (listed in Table 10) and ρ can be used to judge the significance level.In this study, X_A, X_B, X_C are the sets of levels for F-T cycle, carbonation and crack width, respectively. Y is the set of steel corrosion ratio. So the sets of ranks and d_{Y,X_i} can be calculated and listed in Table 11.

Based on the results in Table11, correlation coefficient between each factor and experimental result can be calculated using Eq. (16). The results are listed in Table 12.

As can be seen from Table 9, correlation coefficient between crack width and steel corrosion ratio is the greatest, while carbonation is the smallest. They reveal that crack width possesses the most significant effect on rebar corrosion and carbonation has the least one in these three factors.

In summary, the influence degrees of 3 factors including crack width, carbonation and F-T cycle on rebar corrosion can be ranked by crack width, F-T cycles and carbonation from big to small according to the results of RA, ANOVA and SRCCM. The reasons lie in that cracks are induced by loading, which make carbon dioxide infiltrate along fracture strike in damage layer more easily. The CO_2 can result in a more serious steepness of carbonation front

Table 8
Normalized values of factors and ARSC and corresponding K_{ji}, $\overline{K_{ji}}$.

Factors	Crack width (mm)	F-T cycles (times)	Carbonation time (days)	ARSC (%)
Group 1	−1.15	−1.15	−1.15	−1.75
Group 2	0	0	0	−0.48
Group 3	1.15	1.15	1.15	0.74
Group 4	0	0	−1.15	−0.47
Group 5	1.15	1.15	0	0.88
Group 6	−1.15	−1.15	1.15	−0.87
Group 7	1.15	1.15	−1.15	1.39
Group 8	−1.15	−1.15	0	−0.13
Group 9	0	0	1.15	0.69
K_{j1}	−2.75	−1.49	−0.83	
K_{j2}	−0.26	−0.46	0.27	
K_{j3}	3.01	1.94	0.56	
$\overline{K_{j1}}$	−0.92	−0.50	−0.28	
$\overline{K_{j2}}$	−0.09	−0.15	0.09	
$\overline{K_{j3}}$	1.00	0.65	0.19	

Table 10
Critical value for $N = 9$.

Significance level	0.05	0.01
Critical value	0.600	0.783

Table 11
The results of the ranks and d_{Y,X_i}.

Y	X_A	X_B	X_C	$Rank\ Y$	$Rank\ X_A$	$Rank\ X_B$	$Rank\ X_C$	d_{Y,X_A}	d_{Y,X_B}	d_{Y,X_C}
5.31	0	0	0.00	1	2	2	2	1	1	1
8.52	0	10	0.10	3	2	5	5	−1	2	2
11.62	0	20	0.20	7	2	8	8	−5	1	1
8.56	75	0	0.10	4	5	2	5	1	−2	1
11.97	75	10	0.20	8	5	5	8	−3	−3	0
7.55	75	20	0.00	2	5	8	2	3	6	0
13.26	150	0	0.20	9	8	2	8	−1	−7	−1
9.41	150	10	0.00	5	8	5	2	3	0	−3
11.48	150	20	0.10	6	8	8	5	2	2	−1

Table 12
Spearman's rank correlation coefficient for influence factors.

Factor	X_A	X_B	X_C
Correlation coefficient	0.50	0.10	0.85**

** Correlation is significant at the 0.01 level.

than other health layer and lead to steel bar corrosion easier. Moreover, existence of crack leads to a higher capillarity and osmotic pressure in damage layer. Water and adverse ion solution can infiltrate into concrete more easily. In addition, cracks will aggravate the effect of F-T cycles and chloride penetration. Besides, existence of crack reduces the isolation distance between steel bars and external environment, which make steel bars expose to atmospheric. And existence of crack is helpful for the diffusion of water and oxygen. Cracks lead to a complex synergistic effect of other unfavorable factors.

4. Conclusions

In this paper, the influences of crack width, carbonation and F-T cycles on mass of concrete surface scaling, compressive strength and rebar corrosion are investigated. Experimental scheme is obtained based on orthogonal design, and nine groups of tests need to be carried out. For crack width, it is induced by loading. Three levels of crack width including 0.00 mm, 0.10 mm and 0.20 mm are introduced. For carbonation time, three levels including 0 day, 10 days and 20 days are needed. For times of F-T cycles, three levels including 0, 75 and 100 are conducted. In order to evaluate the properties of concrete, mass of surface scaling is calculated by the data before and after F-T cycles; concrete strength is obtained based on ultrasonic wave velocity and rebound value; and steel corrosion is conducted through the designed electrochemical accelerated method. Following conclusions can be achieved:

(1) Mass of concrete surface scaling possesses positive correlation with times of F-T cycles. However, the growth rate becomes smaller with the increasing of times of F-T cycles. Besides, presence of crack presents enhancement effect.
(2) Compressive strength of concrete possesses negative correlation with times of F-T cycles and decreases by 40% after 150 times of F-T cycles. In addition, the higher value of cracks width is, the higher decrease rate of compressive strength along with F-T cycles presents.
(3) The influences of F-T cycles, carbonation and crack width on steel corrosion ratio are demonstrated based on RA, ANOVA and SRCCM, respectively. According to RA method, R of steel corrosion ratio caused by crack width is 1.68 times of F-T cycle and 4.12 times of carbonation. Based on ANOVA results, the probability of significant effect is over 99% for both crack width and F-T cycles, while the F-Value of crack width is 2.69 times of F-T cycles. Turkey's HSD test and regression analysis results reveal that crack width presents the most significant effect on steel corrosion. For SRCCM, correlation coefficient of crack width is 1.70 times of F-T cycle and much larger than carbonation. As can be concluded through results of these methods, crack width possesses the most significant effect on rebar corrosion, while carbonation possesses the least one.

Acknowledgement

The authors express their appreciation for the financial supports of National Natural Science Foundation of China (Nos. 51408258, 51378236); China Postdoctoral Science Foundation funded project (2014M560237, 2015T80305); Fundamental Research Funds for the Central Universities (JCKY-QKJC06); and Science & Technology Development Program of Jilin Province.

Reference

[1] P. Sharmila, G. Dhinakaran, Compressive strength, porosity and sorptivity of ultra fine slag based high strength concrete, Constr. Build. Mater. 120 (2016) 48–53.
[2] K.S. Youm, J. Moon, J.Y. Cho, J.J. Kim, Experimental study on strength and durability of lightweight aggregate concrete containing silica fume, Constr. Build. Mater. 114 (2016) 517–527.
[3] X. Zhu, G. Zi, Z. Cao, X. Cheng, Combined effect of carbonation and chloride ingress in concrete, Constr. Build. Mater. 110 (2016) 369–380.
[4] H.L. Wang, J.G. Dai, X.Y. Sun, X.L. Zhang, Characteristics of concrete cracks and their influence on chloride penetration, Constr. Build. Mater. 107 (2016) 216–225.
[5] C.G. Berrocal, I. Löfgren, K. Lundgren, L. Tang, Corrosion initiation in cracked fibre reinforced concrete: influence of crack width, fibre type and loading conditions, Corros. Sci. 98 (2015) 128–139.
[6] Y. Zhou, B. Gencturk, K. Willam, A. Attar, Carbonation-induced and chloride-induced corrosion in reinforced concrete structures, J. Mater. Civ. Eng. 27 (2014) 46–70.
[7] L.J. Parrott, D.C. Killoh, Carbonation in a 36 year old, in-situ concrete, Cem. Concr. Res. 19 (1989) 649–656.
[8] S.O. Ekolu, A review on effects of curing, sheltering, and CO_2 concentration upon natural carbonation of concrete, Constr. Build. Mater. 127 (2016) 306–320.
[9] K. Quillin, Modelling Degradation Processes Affecting Concrete, BRE Centre of Concrete Construction, CRC Ltd, 151 Rosebery Avenue, London, 2001. ECIR 4GB. ISBN 1860815316.
[10] F.P. Torgal, S. Miraldo, J.A. Labrincha, J. De Brito, An overview on concrete carbonation in the context of eco-efficient construction: evaluation, use of SCMs and/or RAC, Constr. Build. Mater. 36 (2012) 141–150.
[11] A.A. Sagues, E.I. Moreno, W. Morris, C. Andrade, Carbonation in Concrete and Effect on Steel Corrosion, Final Report, State Job No. 99700-3530-119, WPI

0510685, College of Engineering, University of South Florida, 4202 Fowler Avenue, Tampa, Florida 33620-5350, 1997. p. 299.
[12] R. Heiyantuduwa, M.G. Alexander, J.R. Mackechnie, Performance of a penetrating corrosion inhibitor in concrete affected by carbonation-induced corrosion, J. Mater. Civ. Eng. 18 (2006) 842–850.
[13] R. Liu, L. Jiang, J. Xu, C. Xiong, Z. Song, Influence of carbonation on chloride-induced reinforcement corrosion in simulated concrete pore solutions, Constr. Build. Mater. 56 (2014) 16–20.
[14] V.T. Ngala, C.L. Page, Effect of carbonation on pore structure and diffusional properties on hydrated cement pastes, Cem. Concr. Res. 27 (7) (1997) 995–1007.
[15] P.J. Tumidajski, G.W. Chan, Effect of sulphate and carbon dioxide on chloride diffusivity, Cem. Concr. Res. 26 (4) (1996) 551–556.
[16] J.G. Jang, H.K. Kim, T.S. Kim, B.J. Min, H.K. Lee, Improved flexural fatigue resistance of PVA fiber-reinforced concrete subjected to freezing and thawing cycles, Constr. Build. Mater. 59 (2014) 129–135.
[17] Z. Wang, Q. Zeng, L. Wang, Y. Yao, K. Li, Corrosion of rebar in concrete under cyclic freeze–thaw and Chloride salt action, Constr. Build. Mater. 53 (2014) 40–47.
[18] Y. Qiao, W. Sun, J. Jiang, Damage process of concrete subjected to coupling fatigue load and freeze/thaw cycles, Constr. Build. Mater. 93 (2015) 806–811.
[19] L. Berto, A. Saetta, D. Talledo, Constitutive model of concrete damaged by freeze–thaw action for evaluation of structural performance of RC elements, Constr. Build. Mater. 98 (2015) 559–569.
[20] V.H. Dang, R. François, V. L'Hostis, D. Meinel, Propagation of corrosion in pre-cracked carbonated reinforced mortar, Mater. Struct. 48 (2015) 2575–2595.
[21] P. Lambert, C.L. Page, P.R.W. Vassie, Investigations of reinforcement corrosion. 2. Electrochemical monitoring of steel in chloride-contaminated concrete, Mater. Struct. 24 (1991) 351–358.
[22] F. Shaheen, B. Pradhan, Effect of chloride and conjoint chloride–sulfate ions on corrosion of reinforcing steel in electrolytic concrete powder solution (ECPS), Constr. Build. Mater. 101 (2015) 99–112.
[23] X.Y. Wang, L.N. Zhang, Simulation of chloride diffusion in cracked concrete with different crack patterns, Adv. Mater. Sci. Eng. 2016 (2016) 1–11.
[24] Y. Ji, Y. Hu, L. Zhang, Laboratory studies on influence of transverse cracking on chloride-induced corrosion rate in concrete, Cement Concr. Compos. 69 (2016) 28–37.
[25] S.F. Zhang, C.H. Lu, Y. Chen, Influence of cracks on chloride diffusion and reinforcement corrosion in concrete, Eng. Mech. 01 (2012) 97–100.
[26] D. Niu, Q. Xiao, W. Zhu, Concrete damage and neutralization under coupling effect of carbonation and freeze-thaw cycles, J. Wuhan Univ. Technol. 27 (2012) 353–357.
[27] H. Kuosa, R.M. Ferreira, E. Holt, M. Leivo, E. Vesikari, Effect of coupled deterioration by freeze–thaw, carbonation and chlorides on concrete service life, Cement Concr. Compos. 47 (2014) 32–40.
[28] F.H. Wittmann, P. Zhang, T.J. Zhao, Influence of combined environmental loads on durability of reinforced concrete structures, Int. J. Restor. Build. Monum. 12 (2006) 349–361.
[29] GB/T 50082–2009, National Standard of the People's Republic of China, Standard for methods of long-term performance and durability of ordinary concrete, 2009 (in Chinese).
[30] GB175-2007, National Standard of the People's Republic of China, Common Portland Cement, 2007 (Chinese).
[31] GB 50164–2011, National Standard of the People's Republic of China, Standard for Quality Control of Concrete, 2011 (Chinese).
[32] J. Gao, J. Yin, F. Zhu, X. Chen, M. Tong, W. Kang, J. Lu, Orthogonal test design to optimize the operating parameters of CO_2 desorption from a hybrid solvent MEA-Methanol in a packing stripper, J. Taiwan Inst. Chem. Eng. 64 (2016) 196–202.
[33] W. Zuo, E. Jiaqiang, X. Liu, Q. Peng, Y. Deng, H. Zhu, Orthogonal experimental design and fuzzy grey relational analysis for emitter efficiency of the micro-cylindrical combustor with a step, Appl. Therm. Eng. 103 (2016) 945–951.
[34] J. Tang, G. Gong, H. Su, F. Wu, C. Herman, Performance evaluation of a novel method of frost prevention and retardation for air source heat pumps using the orthogonal experiment design method, Appl. Energy 169 (2016) 696–708.
[35] A. Leyton, R. Pezoa-Conte, A. Barriga, A.H. Buschmann, P. Mäki-Arvela, J.P. Mikkola, Identification and efficient extraction method of phlorotannins from the brown seaweed Macrocystis pyrifera using an orthogonal experimental design, Algal Res. 16 (2016) 201–208.
[36] J. Li, X. Peng, Z. Deng, J. Cao, Y. Guan, L. Lin, Quantitative design on the frost-resistance of concrete, Concrete 12 (2000) 61–65.
[37] JTG D62–2004, National Standard of the People's Republic of China, Code for design of highway reinforced concrete and prestressed concrete bridges and culverts, 2004 (Chinese).
[38] CECS 02: 2005, National Standard of the People's Republic of China, Technical specification for detecting strength of concrete by ultrasonic-rebound combined method, 2005 (Chinese).
[39] X. Wang, X. Liu, C. Zhang, Parametric optimization and range analysis of organic rankine cycle for binary-cycle geothermal plant, Energy Convers. Manage. 80 (2014) 256–265.
[40] O. Keleştemur, S. Yildiz, B. Gökçer, E. Arici, Statistical analysis for freeze–thaw resistance of cement mortars containing marble dust and glass fiber, Mater. Des. 60 (2014) 548–555.
[41] D.C. Montgomery, Design and Analysis of Experiments, eighth ed., Wiley and Sons, New York, 2012.
[42] A. Brown, A new software for carrying out one-way ANOVA post hoc tests, Comput. Methods Programs Biomed. 79 (2005) 89–95.